



Nikolaus Peter Kurt Borowski

**Development of a
Calibration-Free High
Temperature Electrical
Conductivity Measurement for
 CaF_2 Melts and Slag Systems**

**Development of a Calibration Free High-Temperature Electrical
Conductivity Measurement for CaF₂ Melts and Slag Systems**

from the Faculty of Georesources and Materials Engineering of the
RWTH Aachen University

to obtain the academic degree of

Doctor of Engineering Science

approved thesis

submitted by

Nikolaus Peter Kurt Borowski, M.Sc.

Advisors:

Univ. -Prof. Dr.-Ing. Dr. h.c. (UA) Karl Bernhard Friedrich

Prof. Dr. Dr. h.c. mult. Markus Andreas Reuter

Date of the oral examination: 28.10.2022

Schriftenreihe des IME

Band 82

Nikolaus Peter Kurt Borowski

**Development of a Calibration-Free High Temperature
Electrical Conductivity Measurement
for CaF₂ Melts and Slag Systems**

Shaker Verlag
Düren 2023

Bibliographic information published by the Deutsche Nationalbibliothek

The Deutsche Nationalbibliothek lists this publication in the Deutsche Nationalbibliografie; detailed bibliographic data are available in the Internet at <http://dnb.d-nb.de>.

Zugl.: D 82 (Diss. RWTH Aachen University, 2022)

Copyright Shaker Verlag 2023

All rights reserved. No part of this publication may be reproduced, stored in a retrieval system, or transmitted, in any form or by any means, electronic, mechanical, photocopying, recording or otherwise, without the prior permission of the publishers.

Printed in Germany.

ISBN 978-3-8440-8980-6

ISSN 1610-0727

Shaker Verlag GmbH • Am Langen Graben 15a • 52353 Düren

Phone: 0049/2421/99011-0 • Telefax: 0049/2421/99011-9

Internet: www.shaker.de • e-mail: info@shaker.de

Acknowledgements

This thesis is the culmination of many years of work which I could not have completed without the dedication and support of many people. I want to thank:

Prof. Bernd Friedrich for proposing the idea that motivated this work, his support and guidance over the years.

Prof. Markus Reuter who provided excellent suggestions and helped to guide this thesis in its final form.

Franz Hofmann for wonderful and fruitful discussions and his interest and passion for this work.

The curious RWTH undergraduates who assisted me in the lab and added significant value to this thesis: Ralf Rodenbüchler, Hannah Schnitzler, Marco Beckers and Emanuel Drude.

Jürgen Eschweiler for the support and loan of many electrical components and measurement devices.

Amir Kamoush-Koo who was invaluable to me for his support and creativity in designing and manufacturing the cell and measuring periphery.

Tobias Held and his staff, who manufactured the individual molybdenum parts and supported with manufacturing knowledge

Those who read and edited my thesis and made many valuable suggestions.

I would also like to extend to my friends of my office the gratitude I feel towards them:

Lilian Schwich, who was always the cheerful soul of our office, who always had a smile on her face, especially in moments when everything was going wrong.

Ksenija Milicevic-Neumann, who was a valuable and intelligent sparring partner for the technical discussions on cell effects and EIS measurements and made valuable contributions to this work.

Finally, I would like to thank my wife Hanna for her patience, love, and support, who always gave me the courage to persevere, even in difficult times.

For my sons

Contents

Summary.....	I
Extended Abstract.....	III
1 Introduction and Aim of this Thesis.....	1
2 Theoretical Background	3
2.1 Important Thermo-Physical Properties of ESR Slags and their Process Effects	5
2.1.1 Density	5
2.1.2 Surface and Interfacial Tension	5
2.1.3 Viscosity	6
2.1.4 Electrical Conductivity	7
2.1.5 Correlation of Viscosity and Electrical Conductivity.....	9
2.2 Basics of Electrical Conduction	10
2.2.1 Ionic and Electron Conduction.....	11
2.2.2 Electrical Conductivity in Dependence to Slag Composition and Basicity	13
2.2.3 Correlation of Electrical Conductivity with Temperature	14
2.3 The Art of Current: Direct and Alternating Current.....	15
2.3.1 Direct Current	15
2.3.2 Alternating Current.....	17
2.4 Electro-Chemical Cells: The Fundamental System for Electrical Conduction	24
2.4.1 Interfacial Effects	25
2.4.2 Simulation of Electrochemical Cells	29
2.5 Analysis of Electrochemical Systems through Electrochemical Impedance Spectroscopy	29
2.5.1 Measurement Methods.....	29
2.5.2 Plotting the Impedance.....	32
2.5.3 Interpretation of Impedance Plots	33
3 State of the Art: Review of Available Measurement Techniques and Methods ...	37
3.1 Cell Designs and Measurement Techniques	39

3.2	Critical Discussion of Measurement Techniques, Methods and the achieved Results.....	41
4	Research Needs and hypothesis of this work	48
5	The Measurement Technology	50
5.1	The Furnace and the Auxiliary Equipment.....	50
5.1.1	The Linn-Furnace:	50
5.1.2	Vacuum pump station:	51
5.1.3	Inert gas control unit:.....	52
5.1.4	Instrument rack:.....	52
5.2	The Measuring Technique: Cell Design, Setup and Application	53
5.2.1	Material Selection	54
5.2.2	Cell Geometry and Design.....	57
5.2.3	The Application Technique of the Cell.....	63
5.3	Measuring Method: Data Capturing and Processing	67
5.3.1	Cables and Fixture.....	67
5.3.2	Newtons4th LCR Measurement.....	68
5.3.3	Data Plotting and Analysis with ZView™	70
5.3.4	Data Evaluation	71
6	Optimization of the Measuring Accuracy	75
6.1	Influencing Factors on Measurement Accuracy	75
6.2	The Cell Design (Technique)	75
6.2.1	Number of Electrodes	75
6.2.2	Position of Electrodes.....	78
6.2.3	Validation of Calculated Cell Factor (C_f).....	79
6.3	The Measuring Setup (Technique).....	80
6.3.1	Temperature Profile of Furnace and Crucible.....	80
6.3.2	Crucible Insolation	83
6.3.3	Temperature Measurement.....	84
6.3.4	Cable Connection to the Electrodes	85
6.4	Combining Technique with Method	86
6.4.1	Cell Immersion and Immersion Increment	86
6.4.2	Influence of Immersion on the Cell Factor	87

6.4.3	Voltage	87
6.4.4	Frequency Spectrum and Sweep	88
6.5	Electrode Surface Quality and Electrode Surface Cleaning	90
6.6	Data Evaluation (Method)	90
6.6.1	Equivalent Circuit	90
6.6.2	Number of Measurement Points	92
7	Measuring Accuracy Tests – Results and Discussion	94
7.1	Aqueous Solutions	94
7.2	Molten KCl	97
7.3	Molten CaF_2	99
7.4	Critical Discussion of the Achieved Results and Errors	102
7.4.1	Errors through immersion	104
7.4.2	Errors by measurement equipment	105
7.4.3	Fitting Errors	105
7.4.4	Errors due to electrode setup	106
7.4.5	Overall Error	106
8	Limitations of the Measurement Technology	107
8.1	Bottom and Surface Distance	107
8.2	Crucible Effects	109
8.3	Breakdown of Equipotentiality	109
8.4	Equipment Limitations	110
8.5	Immersion Depth and Immersion Increments (precision)	111
9	Conclusion and Future Perspective	115
10	References	117
11	List of Figures	125
12	List of Tables	129
13	Abbreviations and Symbols used in this Thesis	130
14	Appendix	132
14.1	Appendix A: Physical Properties of W and Mo	132
14.2	Appendix B: Mathematical Derivation of Cell Factor	133
14.3	Appendix C: Cable Specification and Data Sheet	134
14.4	Appendix D: Measurement Shunt Options and Related Error	135

14.5	Appendix E: Error due to the Included Resistance caused by the Two Electrode Setup	136
14.6	Appendix F: Calculation of Internal Cell Resistance	137
14.7	Appendix G: Influences of the Skin Effect.....	139
14.8	Appendix H: Certipur® Certifacates.....	141
14.9	Appendix I: Measurement Results	147
14.9.1	KCL.....	147
14.9.2	CaF ₂	154
14.10	Appendix J: Drawings	162
14.11	Appendix K: Example of logarithmic illustration of temperature dependence of the electrical conductivities of melts.....	165

Summary

The specific electrical conductivity of slags is a thermo-physical property that strongly influences the power consumption of metallurgical smelting processes that are based on the principle of resistance heating. Currently, worldwide no measurement technology is available to precisely measure the electrical conductivity of CaF_2 and its slag systems up to high temperatures ($\sim 1,750^\circ\text{C}$). Therefore, the aim of this thesis is to develop a measurement technology that is calibration-free, achieves highest accuracy and stable measurement results over a broad conductivity spectrum up to high temperatures of $\sim 1,750^\circ\text{C}$. The herein developed technology combines well-known best-practice examples, e.g. cell design, measurement technique and measurement method (electrochemical impedance spectroscopy) with an innovative data evaluation process based on simulation of the measurement and fitting of equivalent circuit diagrams to a new measurement technology. The developed technology is evaluated in several aqueous solutions at room temperature, molten KCl and NaCl as well as in molten CaF_2 . The technology is tested on its robustness and calibration-freeness, accuracy and overall measuring error over a wide temperature range from 16°C up to $1,720^\circ\text{C}$ and over an electrical conductivity range starting from 1.356 mS/cm up to $\sim 7\text{ S/cm}$. Finally, the technology limitations are determined and an outlook to further optimization options is given.

Die elektrische Leitfähigkeit ist eine thermophysikalische Eigenschaft, die den Stromverbrauch elektrometallurgischer Schmelz- und Raffinationsprozesse stark beeinflusst. Derzeit ist weltweit keine Messtechnik verfügbar, um die elektrische Leitfähigkeit von CaF_2 und seine Schlackensysteme bis zu hohen Temperaturen ($\sim 1.750^\circ\text{C}$) präzise zu messen. Ziel dieser Arbeit ist es daher, eine Messtechnik zu entwickeln, die kalibrierungsfrei, mit höchster Genauigkeit stabile Messergebnisse über ein breites Leitfähigkeitsspektrum bis hin zu hohen Temperaturen von $\sim 1.750^\circ\text{C}$ ermöglicht. Die hier entwickelte Technologie kombiniert bekannte Best-Practice-Beispiele, z.B. Zelldesign, Messmethode und Messverfahren (Elektrochemische Impedanzspektroskopie) mit einem innovativen Datenauswertungsverfahren basierend auf Simulation der Messung und Fitting von Ersatzschaltbildern zu einer neuen Messtechnologie. Um die Robustheit, Eichfreiheit und Genauigkeit nachzuweisen sowie den Gesamtmessfehler der entwickelten Technologie zu bestimmen, wird diese in wässrigen KCl und NaCl Lösungen bei Raumtemperatur, geschmolzenem KCl und NaCl sowie in geschmolzenem CaF_2 evaluiert. Die Technologie wird dabei über einen weiten Temperaturbereich von 16°C bis 1.720°C sowie über einen elektrischen Leitfähigkeitsbereich von $1,356\text{ mS/cm}$ bis $\sim 7\text{ S/cm}$ getestet. Abschließend werden die Limitationen der Technologie ermittelt und ein Ausblick auf weitere Optimierungsmöglichkeiten gegeben.

Extended Abstract

Introduction

The specific electrical conductivity of slags is a thermo-physical property that strongly influences the power consumption of metallurgical smelting processes that are based on the principle of resistance heating. Even though there have been significant studies on electrical conductivity of slags (see literature and extra reading), literature states no clear value for CaF_2 and CaF_2 based slag systems at elevated temperatures. The wide range of electrical conductivities for CaF_2 that was measured and are stated in literature are shown in Figure 1. Furthermore, currently no measurement technology is available that can accurately measure the electrical conductivity of CaF_2 or CaF_2 -based slag systems at the temperatures of their usual application. Therefore, this thesis solely focuses on the development of a measurement technology that is feasible of measuring the electrical conductivity of molten CaF_2 and its slag systems.

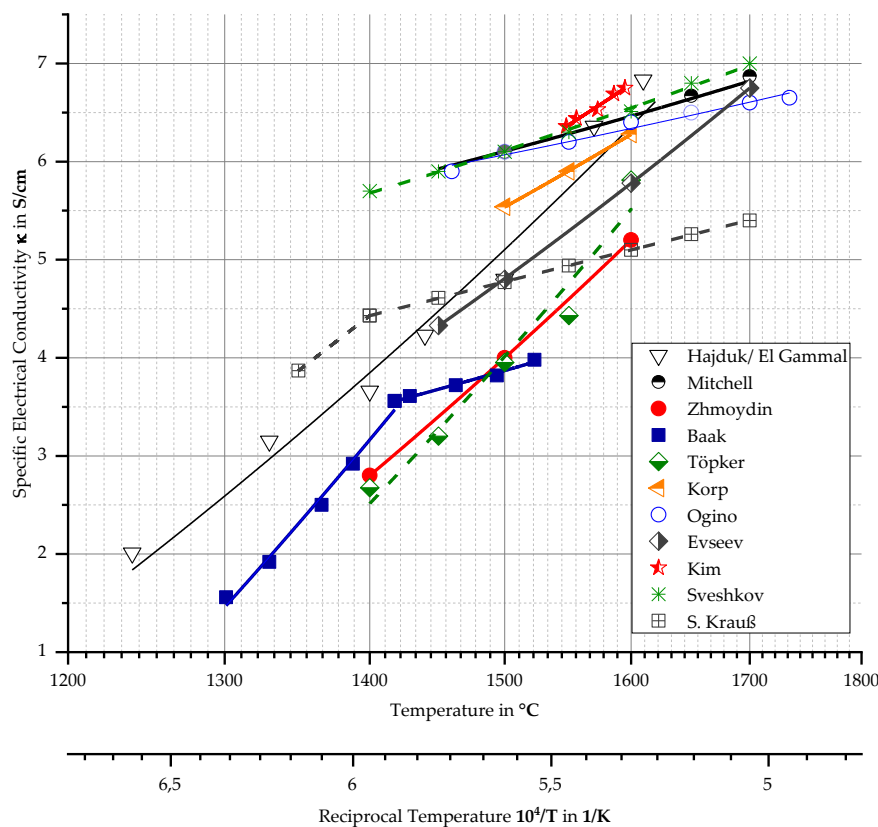


Figure 1: Electrical conductivity of CaF_2 versus the temperature of various references and cell designs

Due to the lack of measurement technology in addition to the scarce and deviating high temperature results a measurement technology and method has been developed in this thesis. It should be calibration-free, achieve highest accuracy and yield stable as well as reproducible specific electrical conductivity results. Therefore, the technology should be able to cover a broad conductivity spectrum starting at the value of mS/cm

and range up to 7,5 S/cm. Furthermore, it shall be applicable at high temperatures up to ~1,750°C.

Fundamentals

The electrical conductivity or conductance describes the physical capability of a material to conduct electric current. From a microscopic point of view electrical conduction can be seen as the ability of a material to transport charge in its inner phase through moving electrons or ions. This can either be driven by an outer force like an electric field due to an electric potential difference, or by concentration gradient inside the material itself. It is essentially determined by the available number of charge carriers, their charge and movability. Regardless the nature of the current transport all conducting materials can be characterized by an uniform dimensioning system. The basic properties are:

- resistance R in Ω (Ohm)
- conductance G in S (Siemens)

whereas the conductance G cannot be directly measured and therefore is described by the reciprocal value of measured resistance:

$$G = \left(\frac{1}{R}\right) \quad (1)$$

With the knowledge of voltage and current, the resistance of a conductor can be determined according to Ohm's law

$$U = R \cdot I \rightarrow R = \frac{U}{I} \quad (2)$$

and subsequently the conductance of a material by forming the reciprocal value of the determined resistance. But with changing length or cross-sectional area of the conductor also the electrical conductivity will change and therefore the conductance. Although it becomes apparent that the conductance gives us a good idea of how well the material conducts the current, it still says nothing about the absolute electrical conductivity of the material. Therefore, the defined geometric dimensions of length and cross-sectional area of the conductor that led to the measured resistance are necessary. If both are known in detail, the specific electrical conductivity can be determined according to:

$$\kappa = G \cdot \left(\frac{l}{A}\right) = G \cdot Cf \quad (3)$$

The specific electrical conductivity κ (in $S \cdot m/mm^2$ for solid materials and S/cm for liquids) and the specific resistance ϱ (in $\Omega \cdot mm^2/m$ or $\Omega \cdot cm$) state the absolute and size independent values of a material. [14, 15] In terms of liquid materials the relating factor $\left(\frac{l}{A}\right)$ is named "cell-factor" and is a key parameter of conductivity measurements of liquid or molten materials. Here "l" stands for the distance between the cell electrodes

while “A” is equal to the cross-sectional area that the cations/anions must pass through. [16]

Since slags at elevated temperatures are disintegrated into cations and anions, they any measurement that uses direct current would lead to false results due to a separation and concentration of the ions. Hence alternating current must be applied for the determination of the specific electrical conductivity. In contrast to DC-circuits the direction of charge motion of AC-circuits periodically reverses. In the simplest case the form of current (voltage) is that of a sinewave and may be written as

$$i(t) = \hat{i} \cdot \sin(\omega t + \varphi_i) \quad (4)$$

$$v(t) = \hat{v} \cdot \cos(\omega t + \varphi_u) \quad (5)$$

where $i(t)$ ($v(t)$) is the value of current (voltage) at time t , \hat{i} (\hat{v}) the maximum of current (voltage) which simultaneously is the “amplitude” and ωt a frequency-based time variable that is added to an initial phase shift φ_i (φ_v) between current and voltage. Using alternating currents Ohm’s law is still applicable but the simple resistance becomes a value of complex nature and is named impedance:

$$v(t) = Z(t) \cdot i(t) \quad (6)$$

The impedance is composed of a real part Z' and an imaginary part Z'' and can be expressed as [20, 26, 28]

$$Z = Z' + Z'' = R + j \cdot X_c \quad (7)$$

where R (Z') is the real and $j \cdot X_c$ (Z'') is the imaginary part. Hereby R is called the resistance and X the reactance of the system. The absolute magnitude of the impedance, equivalent to the length of the impedance vector Z , is defined by [20, 26, 28]

$$|Z| = \sqrt{Z'^2 + Z''^2} \quad (8)$$

To obtain pure electrical conductivity values of any device under test, it is necessary to extract the purest resistance R possible out of the complex value of Z .

Measurement Technology

Since liquids do not form a stable and easily definable geometric size of which the electrical resistance could be measured, a measurement device also called “electrochemical cell” is needed to define the frame of reference for the measurement to be conducted. The cell is composed of a container, which can be neglected for the following discussion since any kind of container is needed to hold the liquid, and a measurement device, which consists of at least two electrodes that are immersed into the liquid. Depending on the art and design of the electrodes the current paths between the two electrodes propagate differently. If the current paths are well defined by the geometrical shape of the cell and independent of the electrical properties of the liquid under test, it is referred to as high accuracy cell, which needs no calibration. In all other

cases the cell is referred to as cell of low accuracy and does need a calibration for the correct determination of the cell factor. To be calibration free a cell of high accuracy has been developed based on the ring cell type with a retracted center electrode.

The entire design of the measuring cell has been developed with maximum flexibility and robustness in mind. This means the cell is designed in such a way that the center electrode can always be easily and constantly centered and is not inadvertently moved out of position. The individual components are easily replaceable when it comes to maintenance or system modifications such as changing the cell factor. To be able to vary the cell factor, the outer ring electrode is designed to be exchangeable, so that different ring sizes can be installed quickly. To meet all these requirements, the measuring head which consists of three main parts (high temperature parts, low temperature parts and insulating parts) as shown in Figure 2, is divided into four different sections.

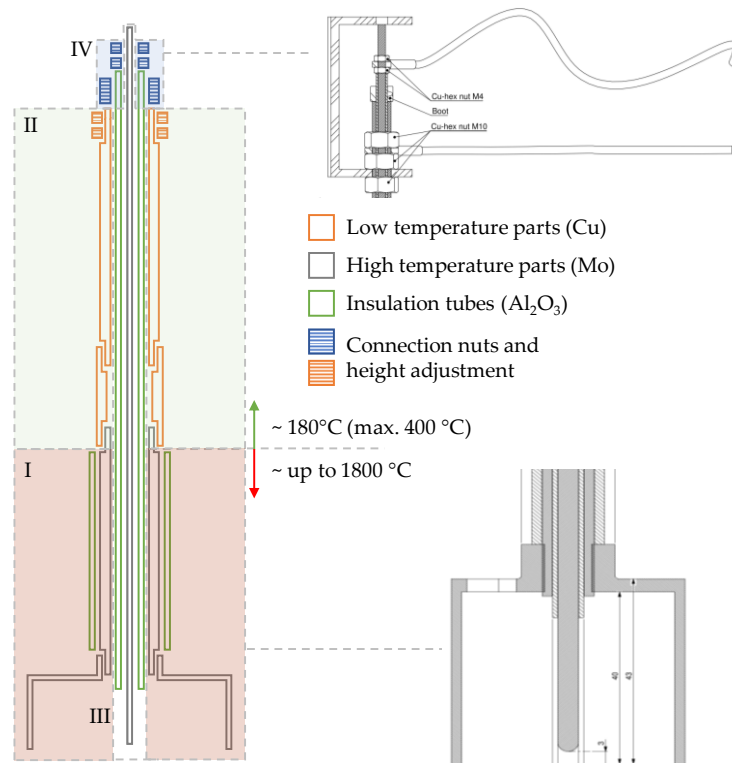


Figure 2: Schematic illustration of the entire measurement head (not to scale); I): High temperature molybdenum part; II): Low temperature copper part; III): Center electrode with IV): height adjustment

Due to the large temperature difference between the inner heating chamber and the other inner parts of the furnace, the first part, consisting of the outer ring electrode and its extension to the device holder, is divided into the sections I) and II). This has the following reason: while the temperatures in the outer furnace part are moderate, the temperatures in the inner heating area are up to 1,750 °C and very demanding in terms of material properties. Parts that must withstand these high temperatures and the

extreme temperature fluctuations while immersed into the inner part of the furnace, are exposed to extreme conditions, and change their material properties over time. This results in microcracks and material failure. For this reason, the ring electrode and its extension in section I) are made of molybdenum and are designed so, that they can be quickly replaced. All parts in section II), i.e. above the heat shield, are situated in the lower temperature range and can therefore be made of copper. The second main part of the measuring head is section III), which consists of the center electrode and its insulation. To always position the center electrode reproducible and stable in the center of the ring electrode, it is guided centrically in the inner of the extension tubes of the outer electrode into the ring electrode. Due to this design, the center electrode cannot be divided into two parts like the outer electrode and must therefore be consistently designed for the highest temperatures. Thus, the center electrode and its insulation extend uninterruptedly from the low temperature areas to the high temperature areas as the center of the entire measurement setup. The last main part is section IV), which contains a special screw mechanism for height adjustment of the center electrode relative to the ring electrode as well as the attachment of the measuring leads. All four parts are described individually in detail in the thesis.

The height of the center electrode can be adjusted by copper nuts. The nuts rest firmly on the protective tube of the center electrode, which is always held in position by a sleeve with grub screw. The sleeve in turn rests firmly on an insulating aluminum oxide spacer plate on the copper extension of the ring electrode. Thus, the aluminum oxide protective tube of the center electrode is fixed in position with respect to the ring electrode. Thus, the position of the center electrode relative to the lower edge of the ring electrode can be screwed higher or lower based on this mechanism. For all measurements, the center electrode is retracted 3 mm to stabilize the electric field inside the ring electrode and reduce the lower edge field according to the results of previous test measurements. Assuming that the electrodes are perfectly conductive, the radial electric field between the electrodes of a coaxial cell can be calculated according to Maxwell's law, similar to the calculation of a cylindrical capacitor. The resistance through the cell with the radii a for the center electrode and b for the ring electrode and corresponding length, which equals the immersion depth z , can be calculated according to [93]:

$$R = \frac{V}{I} = \frac{1}{\kappa} \cdot \frac{\ln\left(\frac{b}{a}\right)}{2\pi} \cdot \frac{1}{z} \quad (9)$$

Although the measurement cell is a cell of high accuracy per definition, in real measurements, however, surface- and bottom fringe fields occur in addition to the radial section as indicated in Figure 3. In both fringe fields the current paths are not solely defined by the geometrical dimensions of the cell and would falsify the measurement if neglected.

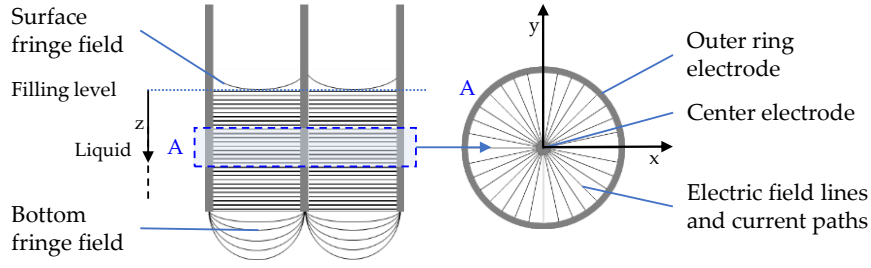


Figure 3: Coaxial electrode cell with corresponding electric field lines and current paths

A suitable technique to address this fringe fields and exclude them from the measurement is described by Schiefelbein in [58]. The impedance of the liquid is measured in parallel to the impedance caused by the fringe fields so that the total real part $R_{liq.}$ of the measured impedance can be expressed by

$$\frac{1}{R_{liq.}} = \frac{1}{R_{radial,liq}} + \frac{1}{R_{fringe}} \quad (10)$$

where $R_{radial,liq}$ is the real part of the radial constant part between the two electrodes and R_{fringe} the real part of the surface- and bottom fringe fields. Since the fringe fields in the same liquid remain constant at various immersion depths, the resistance R_{fringe} can be separated and removed from the total resistance $R_{liq.}$ by subtracting one measurement from the other according to

$$\kappa = \left(\frac{\ln \left(\frac{b}{a} \right)}{2\pi} \right) \cdot \left(\frac{1}{z_1 - z_2} \right) \cdot \left(\frac{1}{R_{liq.,1}} - \frac{1}{R_{liq.,2}} \right) \quad (11)$$

In differential form equation 11 can be written as: [based on [60]]

$$\kappa = \left(\frac{\ln \left(\frac{b}{a} \right)}{2\pi} \right) \cdot \frac{1}{dz} \cdot d \left(\frac{1}{R_{liq.}} \right) = \left(\frac{\ln \left(\frac{b}{a} \right)}{2\pi} \right) \cdot \frac{d \left(\frac{1}{R_{liq.}} \right)}{dz} = Cf^* \cdot m^* \quad (12)$$

From equation (12) can be seen that the electrical conductivity is determined from a constant part Cf^* (Cf^* excludes the immersion dimension z) of the cell factor Cf and the differential term of $\frac{d \left(\frac{1}{R_{liq.}} \right)}{dz}$. $\frac{d \left(\frac{1}{R_{liq.}} \right)}{dz}$ can be considered as an expression of the slope m^* of the graph of the plotted values of $\left(\frac{1}{R_{liq.}} \right)$ versus dz . This expression, as illustrated in Figure 4, shows that the plotted readings from different immersion depths must be strictly linear.

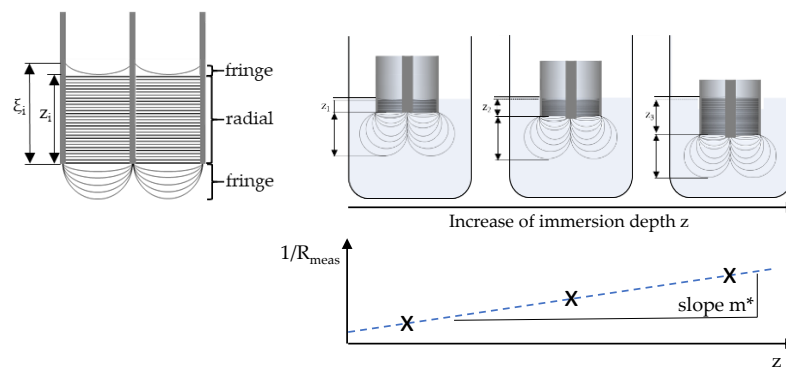


Figure 4: Schematic representation of radial and fringe current paths at different immersion depths

To obtain the pure radial resistance of the electrolyte from the measured complex impedance of the cell electrochemical impedance spectroscopy is used. Therefore, a phase sensitive multimeter (PSM1735 of Newtons4th) is used to conduct a frequency sweep of 32 measurement points that are equally spread over a frequency range from 500 Hz to 150 kHz. To minimize stray effect and insulate the load effects of the PSM outputs from the measurement an additional impedance analysis interface is connected in series to the PSM. During the measurement the PSM determines the real and imaginary components of the systems response at a fundamental frequency using DFT analysis by dividing the voltage ($a + jb$) and the current signal ($c + jd$), into their real and imaginary parts. From these fundamental compounds the complex impedance is computed and subsequently visualized with ZView™. To determine the pure real part R_{liq} of the measured impedance spectrum, the recorded data must be modeled using an equivalent circuit which mirrors the real measurement cell. Therefore, the typical electrical components such as resistors, capacitors and inductors, as well as some components that have no electrical analog such as constant phase elements and Warburg impedances are arranged in a meaningful order and then matched to physical characteristics of the measured cell. Once a suitable equivalent circuit has been developed each element of the circuit is fitted so that the simulated result matches the real measurement as good as possible. A fitting example of an exemplary measurement with fitting deviation of the individual components and the determined final pure value for the resistance of the liquid in the radial section of the electrodes is shown in Figure 4.

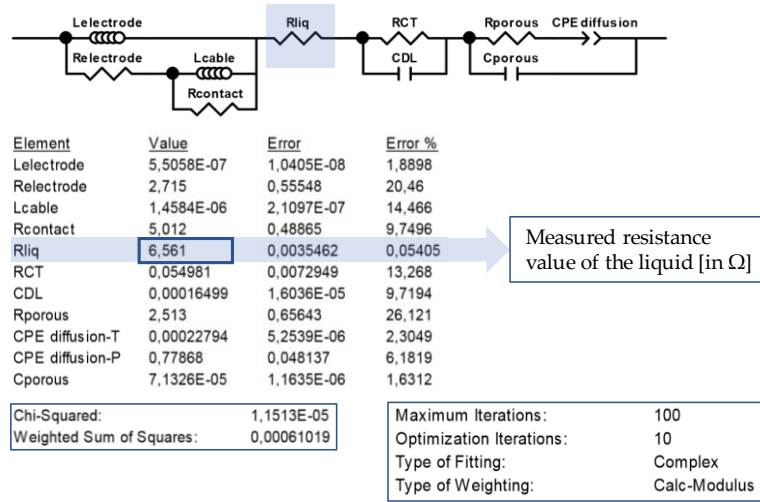


Figure 5: Exemplarily illustration of a fitting result with fitting deviation

During the first conducted test measurements with the ring cell, it could be identified that the modified and adapted equivalent circuit developed from literature shows increasingly bad results with increased electrical conductivities. This can be explained with the increase in number of ions that take place in carrying charge and therefore change the reactions of the system at the electrode/electrolyte interface. Hence, it is obvious that the equivalent circuit must be further modified for measurements of increased electrical conductivity. It has been identified that the applicable measurement range can be divided into three characteristic sections of similar electrochemical reactions to the system. These are:

- Aqueous solutions with conductivities $\kappa < 500 \text{ mS/cm}$
- Liquid salts and slags with conductivities $500 \text{ mS/cm} \leq \kappa \leq 2.49 \text{ S/cm}$
- Liquid salts and slags with conductivities $\kappa > 2.5 \text{ S/cm}$

The deviation of the individual equivalent circuits of the three sections is mainly based on increased ion content and increased movability in the liquid phase. This changes the electrochemical response of the system to alternating current. With increasing ion content and thereby increasing electrical conductivity the measurement dominating part switches from the capacitive double layer to the inductive part of the measurement. In terms of equivalent circuit modeling this means, that the dominating double layer effects are reduced while the inductive reaction effects become dominating at higher conductivities. The resulting equivalent circuit models are shown in Figure 7 to Figure 8.

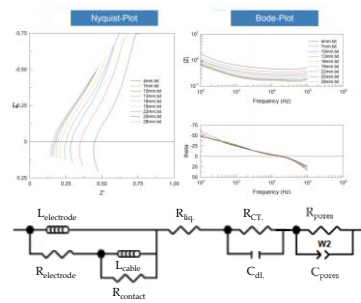


Figure 6: Equivalent circuit for conductivities $\kappa < 500$ mS/cm (e.g. aqueous solutions)

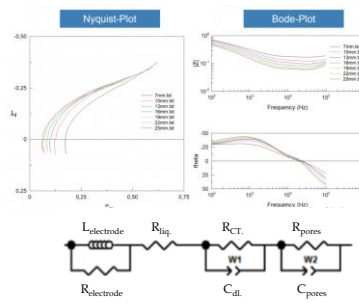


Figure 7: Equivalent circuit for conductivities $500 \text{ mS/cm} \leq \kappa \leq 2.49 \text{ S/cm}$ (e.g. liquid salts)

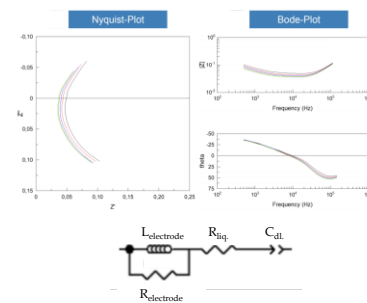


Figure 8: Equivalent circuit for conductivities $\kappa > 2.5$ S/cm (e.g. liquid slags/salts)

To precisely evaluate the measurement and fitting results obtained, the inversed values of the determined real components of the liquid's resistance are plotted against the corresponding immersion depth z as shown in Figure 9. The resulting slope of the linear regression line of the plotted data points is then multiplied with the constant part of the cell factor Cf^* . The product yields the specific electrical conductivity of the liquid under test. Based on the accuracy of the regression line and the linearity of the plotted measurement points, the quality of the result can be evaluated, and potential errors or deviations can be determined and explained.

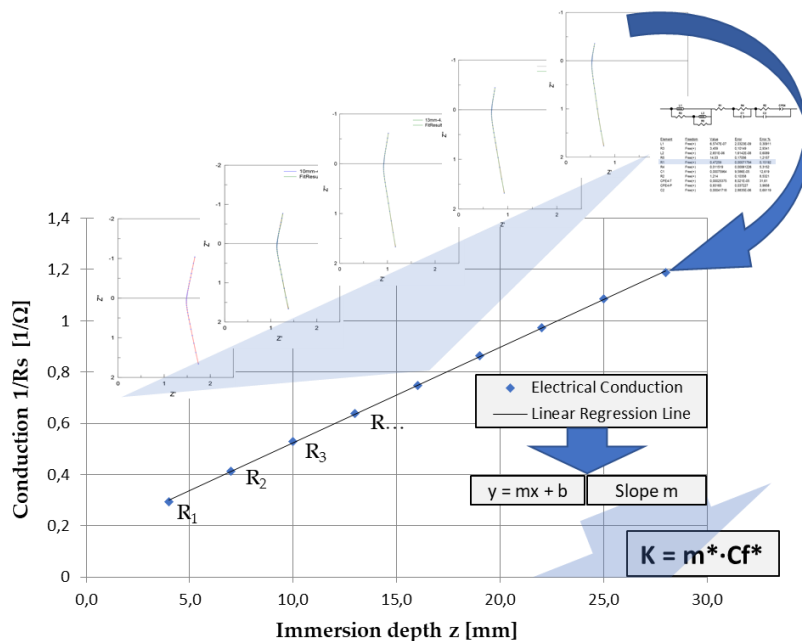


Figure 9: Schematic illustration of measurement method: 1) Several measurements are conducted at various immersion depth z ; 2) the reciprocal resistance of the fitting results of these measurements are plotted over the immersion depth; 3) the slope of the regression line multiplied with the geometric cell factor Cf^* gives the specific electrical conductivity of the measurement

Experimental

Before the measurement technology was applied to measure CaF_2 the system was validated with aqueous solutions (NaCl and KCl), to test its functionality at low temperatures and low conductivities, and with molten KCl, to test the functionality up to temperatures of 1,000 °C and electrical conductivities up to 2,7 S/cm. In the following only the results of KCl will be exemplarily shown to prove the functionality of the measurement technology. Detailed results can be seen in the thesis. The achieved results are stated in Table 1.

Table 1: Measurement results of aqueous KCl solutions at room temperature and their deviation from literature values (evaluated from [98])*

KCl Solutions	5 wt. %	10 wt. %	15 wt. %	20 wt. %
Measured κ [in mS/cm]	74.66	143.28	207.46	264.96
Temperature [in °C]	22	20	20	18.5
Ref. κ (20°C) [98, 99] [in mS/cm]	71.9	143.0	208.0	271.6*
Deviation	3.8%	0.2%	-0.3	-2.5%
Ref. κ with temp. correction	74.78	143.00	208.00	263.45
Deviation	-0.16%	0.20%	-0.26%	0.57%

To prove the measured values, they are compared to literature values from [98, 100] which were determined by using a capillary method and are therefore considered as precise reference values for a specified norm temperature of 20 °C. The temperature deviation will be compensated by a temperature correction equation derived from literature. Comparing the corrected values to the measured values, an accordance with a deviation of below 1 % can be identified.

To expand the measurement tests to higher temperatures and to higher electrical conductivities the aqueous solutions are replaced by KCl. The molten salt is investigated between 860 °C up to 1,050 °C and the temperature dependent specific electrical conductivity of molten KCl is determined over this temperature range. To identify the measurement method's accuracy at these elevated temperatures and increased electrical conductivities, the achieved values are compared to literature.

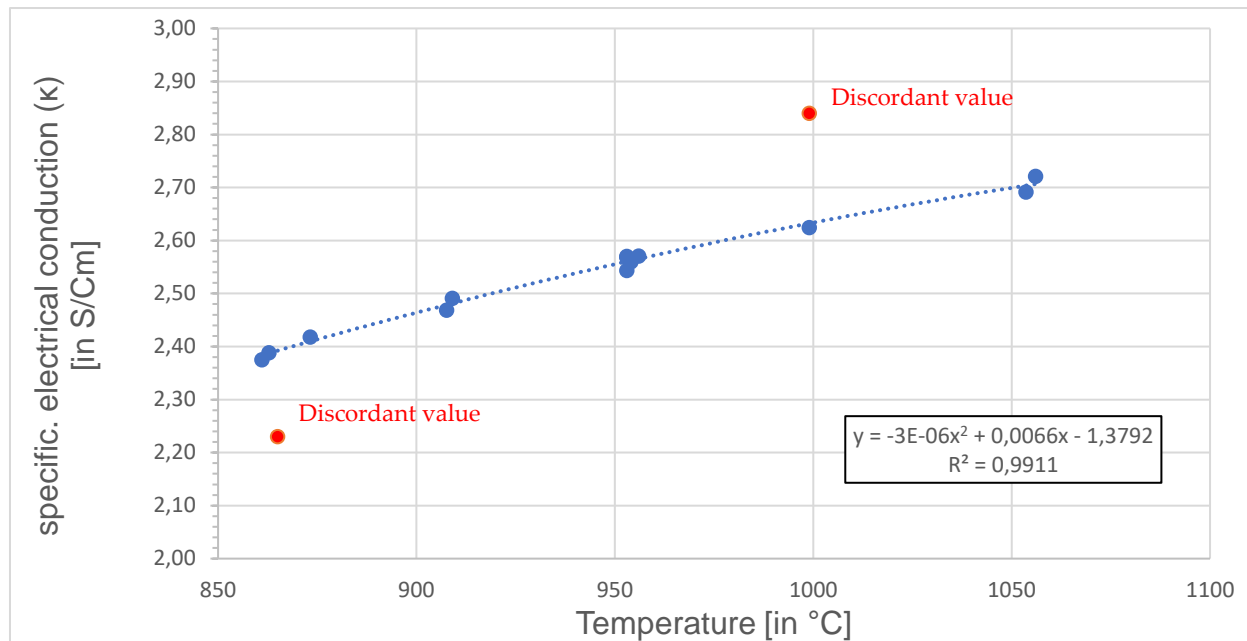


Figure 10: Specific electrical conduction measurement results of molten KCl in dependence to temperature

The determined electrical conductivity values of various measurements over the temperature range from 860 °C to 1050 °C are illustrated in Figure 10. To assess the temperature dependent measurement results, the individual measurement values as well as the entire measurement over the given temperature range will be compared to the literature values determined by van Artsdalen and Yaffe in [99]. Therefore, the plotted values are fit with a polynomic regression line of second order. Table 3 states the individual measurement results in comparison to the literature values of van Artsdalen and Yaffe. The determined electrical conductivity values are in good accordance with the values stated by van Artsdalen and Yaffe and show a maximum deviation of below 1 %.

Table 2: Extract from the measurement results of the temperature dependent electrical conductivity of molten KCl

Temperature dependent electrical conductivity of molten KCl											
Measured κ [in S/cm]	2.38	2.39	2.42	2.47	2.49	2.56	2.57	2.57	2.62	2.69	2.72
Temperature [in °C]	861	863	873	908	909	953	953	956	999	1054	1056
Ref. κ [97] [in S/cm]	2.38	2.39	2.41	2.48	2.48	2.56	2.56	2.57	2.63	2.70	2.70
Deviation	0.0%	0.0%	0.4%	-0.4%	0.4%	0.0%	0.4%	0.0%	-0.4%	-0.4%	0.8%

After proving the temperature resistivity, stability and high accuracy of the measurement cell and method, the final test and originally intended measurement of

molten CaF_2 was conducted at temperatures in between 1,438 °C and 1,710 °C to measure the highest possible electrical conductivity that the herein developed system is intended to. The achieved measurement results are plotted in Figure 11.

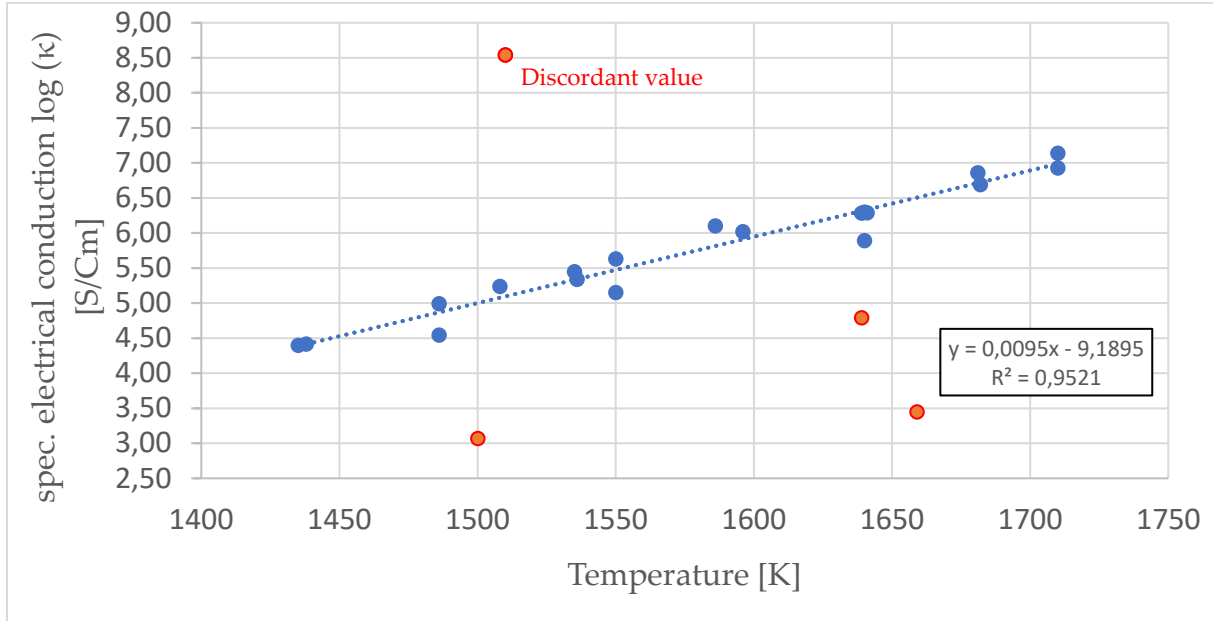


Figure 11: Determined temperature dependent specific electrical conductivity of molten CaF_2 between 1,430 °C and 1,720 °C with linear regression line and discordant values

For the CaF_2 measurements an increased deviation of individual measurement points can be identified. Even the scattering of multiple conducted measurements at the same temperature is strongly increased compared to the measurements within aqueous solutions or molten KCl . To evaluate the measurement precision and the deviation of the individual measurements, a regression line is drawn through the obtained measurement results excluding the discordant values (values are not considered because of the significant and far to big deviation in comparison to the other measurements) marked red in Figure 11. Based on the resulting formula of this regression line, specific electrical conductivity values can be generated and compared to literature. From the conducted measurements the following regression line is obtained:

$$\kappa(T) = 0.0095 \cdot T - 9.3159 \quad (13)$$

with $\kappa(T)$ the calculated, temperature dependent specific electrical conductivity and T the temperature in °C. The detailed deviation of the individual measurement values from the values calculated using the regression line formula are shown in Table 3. A maximum deviation of 6.1 % of the individual conducted measurements was identified. To assess the obtained results and the order of magnitude, the results were compared with meaningful literature values. The obtained values are in between the literature values.

Table 3: Deviation of the individual measurements and the discordant values from the determined regression line at a selected temperature of 1,640 °C

	Measurement Values												Discordant Values			
Temperature [in °C]	1,438	1,486	1,486	1,536	1,586	1,586	1,639	1,640	1,640	1,641	1,710	1,710	1,510	1,585	1,639	1,659
κ measured [in S/cm]	4.41	4.55	4.99	5.34	6.1	5.7	6.28	6.30	5.89	6.29	6.39	7.14	8.54	3.07	4.79	3.45
calculated κ [in S/cm] according to regression line	4.35	4.8	4.8	5.28	5.75	5.75	6.25	6.25	6.26	6.27	6.93	6.93	5.03	5.74	6.25	6.44
Deviation	1.5 %	5.2%	3.9%	1.1%	6.1%	-0.9%	0.4%	0.6%	-6.0%	0.3%	0.0%	3.0%	69.8%	-46.5%	-23.4%	-46.5%
Standard Deviation							0.2002									
Deviation in %							3.2%	3.2%	3.4%	3.2%						

While different literature results either on the high temperature side or on the low temperature side show a good accordance with the determined values, the values determined by Evseev show a very high overall accordance with the measured results, as shown in Table 4.

Table 4: Comparison of determined electrical conductivity values of molten CaF_2 with literature.

	1,450 °C	1,500 °C	1,550 °C	1,600 °C	1,700 °C
	Specific Electrical Conductivity κ of CaF_2 [in S/cm]				
Own measurements	4.46	4.93	5.41	5.88	6.83
Korp	-	5.54	5.90	6.28	-
Töpker	3.19	3.95	4.40	5.80	-
Ogino	5.90(1,460)	6.10	6.20	6.40	6.60
Hajduk	4.50	4.80	6.36 (1,570)	6.83 (1,610)	
Evseev	4.33	5.00	-	5.78	6.75

Even though the measured values of Evseev are slightly smaller, they show a relatively constant deviation of the individual measurement values of only -3.0 % to -1.2 %.

Conclusion

The herein developed technology was tested in several aqueous solutions, molten KCl and molten CaF_2 , in a temperature range from 16 °C up to 1,720 °C, and an electrical conductivity range starting from 1.356 mS/cm up to ~7,2 S/cm. The technology proved to be stable and calibration-free and showed high accuracy and low errors. It can be concluded that the developed measurement technology fulfills all previously set requirements and is able to accurately measure and determine the specific electrical conductivity of ESR slags up to high process temperatures of 1,720 °C. To further improve the stability and accuracy especially at high temperatures and conductivities, the cell should be further optimized so that the cell factor is increased, and the resistance of the cell decreased. This would lead to more stable and accurate measurements at elevated conductivities and temperatures.